JOURNAL OF ENVIRONMENTAL SCIENCES 90 (2020) 234–243

Available online at www.sciencedirect.com

ScienceDirect

www.elsevier.com/locate/jes

JES JOURNAL OF ENVIRONMENTAL SCIENCES

www.jesc.ac.cn

Release of deposited MnO_2 nanoparticles from aqueous surfaces

Hainan Wang [1], *Ruixing Huang* [1], *Chengxue Ma* [1], *Xiaoling Li* [2], *Caihong Liu* [1], *Qiang He* [1], *Zhengsong Wu* [1], *Jun Ma* [3], *Xiaoliu Huangfu* [1,*]

[1] *Key Laboratory of Eco-environments in Three Gorges Reservoir Region, Ministry of Education, College of Environment and Ecology, Chongqing University, Chongqing 400044, China*

[2] *Key Laboratory of Water Supply and Sewage Engineering, Ministry of Housing and Urban-Rural Development, School of Civil Engineering, Chang'an University, Xi'an 710054, China*

[3] *State Key Laboratory of Urban Water Resource and Environment, School of Municipal and Environmental Engineering, Harbin Institute of Technology, Harbin 150001, China*

ARTICLE INFO

Article history:
Received 29 August 2019
Received in revised form
17 December 2019
Accepted 17 December 2019
Available online 31 December 2019

Keywords:
QCM-D
Release kinetics
MnO_2 nanoparticles (MnO_2 NPs)
Solution pH
Biomacromolecule

ABSTRACT

Changes in solution chemistry and transport conditions can lead to the release of deposited MnO_2 nanoparticles from a solid interface, allowing them to re-enter the aqueous environment. Understanding the release behavior of MnO_2 nanoparticles from naturally occurring surfaces is critical for better prediction of the transport potential and environmental fate of MnO_2 nanoparticles. In this study, the release of MnO_2 nanoparticles was investigated using a quartz crystal microbalance with dissipation monitoring (QCM-D), and different environmental surface types, solution pH values and representative macromolecular organics were considered. MnO_2 nanoparticles were first deposited on crystal sensors at elevated $NaNO_3$ concentrations before being rinsed with double-deionized water to induce their remobilization. The results reveal that the release rate of MnO_2 depends on the surface type, in the decreasing order: $SiO_2 > Fe_3O_4 > Al_2O_3$, resulting from electrostatic interactions between the surface and particles. Moreover, differences in solution pH can lead to variance in the release behavior of MnO_2 nanoparticles. The release rate from surfaces was significantly higher at pH 9.8 that at 4.5, indicating that alkaline conditions were more favorable for the mobilization of MnO_2 in the aquatic environment. In the presence of macromolecular organics, bovine serum albumin (BSA) can inhibit the release of MnO_2 from the surfaces due to attractive forces. In presence of humic acid (HA) and sodium alginate (SA), the MnO_2 nanoparticles were more likely to be mobile, which may be associated with a large repulsive barrier imparted by steric effects.

* *Corresponding author.*
E-mail address: hfxl@cqu.edu.cn (X. Huangfu).

https://doi.org/10.1016/j.jes.2019.12.011

Introduction

MnO_2 nanoparticles (MnO_2 NPs) are nanosized manganese oxides commonly found in both natural and anthropogenic aquatic environments through the natural processes of mineral weathering or anthropogenic processes of manganese (Mn(II)) oxidation or permanganate (Mn(VII)) reduction (Buffle and Leppard, 1995; Ma and Graham, 1996; Wigginton et al., 2007). The application of MnO_2 NPs has been increasingly reported for the removal of contaminants due to their high surface activity, allowing them to act as oxidants or adsorbents (Jiang et al., 2009; Huangfu et al., 2017a; Huangfu et al., 2017b; Marafatto et al., 2018), and they inevitably recharge into the aquatic environment and influence other co-existing pollution (e.g., organic and metal). In most cases, MnO_2 NPs can attach to aquatic surfaces, while under adverse conditions, the deposited MnO_2 NPs can be released from the nature surfaces of sand, rocks, or sediments as the solution conditions rapidly change (e.g., during storms and floods) (Torkzaban et al., 2013; Yi and Chen, 2013; Chowdhury et al., 2014b). Once the release takes place, MnO_2 NPs can return into the aqueous phase and thereby influence the transport of themselves and the relevant pollution. Therefore, understanding the reversibility of MnO_2 NP retention on naturally occurring surfaces is crucial for a better control of their mobility and environmental fate in aquatic systems.

The deposition and release behaviors of MnO_2 NPs are considered two key processes codetermining the mobility of MnO_2 NPs suspended in aqueous environments (Huangfu et al., 2019; Jean et al., 1996; Markus, 2016). The deposition kinetics of MnO_2 NPs on representative environmental surfaces have been investigated previously and can be qualitatively explained by Derjaguin-Landau-Verwey-Overbeek (DLVO) theories (Huangfu et al., 2019). Electrostatic surface properties play an important role in controlling MnO_2 colloidal deposition on different surfaces in monovalent sodium solutions. The significant high energy barrier calculated for MnO_2 NPs with similarly negative silica and magnetite surfaces in the study indicated that the retention of MnO_2 under those unfavorable conditions may be reversible and that MnO_2 NPs were likely to be released back into the aqueous phase. However, under the favorable conditions for MnO_2 deposited onto the alumina surface, the deposition may be irreversible due to the existence of attractive forces (Huangfu et al., 2019).

Extensive research has been conducted on the release of nanoparticles by performing a quartz crystal microbalance with dissipation monitoring (QCM-D) technique (Quevedo and Tufenkji, 2009; Yi and Chen, 2013; Yi and Chen, 2014; Chowdhury et al., 2014b; Wang et al., 2017). With the properties of high sensitivity and low sample volume requirements, QCM-D can be a useful tool for determining the interaction of nanomaterials with interfaces. Yi and Chen (2013) reported that multiwalled carbon nanotubes (MWNTs) deposited on flat silica surfaces can be released when the background Na^+ or Ca^{2+} concentration is decreased at pH 7.1. Similarly, Chowdhury et al. observed the remobilization of deposited graphene oxide (GO) from silica-coated QCM crystal surface when rinsed with deionized (DI) water (Chowdhury et al., 2014a). The release of nanoparticles in these studies is considered occur at the primary energy minimum due to the parallel-plate flow in the QCM chamber only allowing for nanoparticle deposition at the primary energy minimum (Yi and Chen, 2013; Yi and Chen, 2014). Although many studies have been conducted on the release behavior of nanoparticles from silica surfaces, research on their release from different surfaces is still limited. Moreover, molecular organic matter (e.g., humic substances, polysaccharide and protein), which is widely present in natural environments, can significantly impact the stability and mobility of MnO_2 NPs and thus affect the release and detachment of deposited MnO_2 NPs from interacting surfaces. While those environmental factors are critical for the interaction of MnO_2 NPs with surfaces, work on release behavior of MnO_2 NPs from environmental surfaces under relevant conditions has not yet been established.

In this study, the release behavior of deposited MnO_2 NPs from crystal surfaces in monovalent sodium nitrite was investigated using a QCM-D. MnO_2 NPs were first deposited on crystal surfaces in the background electrolytes and then exposed to double-deionized (DDI) water to induce the release of MnO_2. The typical coatings (e.g., silica, magnetite, or alumina) of crystal sensors, which represent the model mineral surfaces that may be encountered by migrating MnO_2 NPs, were chosen to examine the influence of surface type on the reversibility of MnO_2 deposition. The effect of solution pH and molecular organic matter on the release of deposited MnO_2 from evaluated surfaces was also investigated.

1. Materials and methods

1.1. MnO_2 NPs synthesis and characterization

The synthetic method for MnO_2 NPs in this study was identical to the approach utilized in our previous publications (Huangfu et al., 2013; Huangfu et al., 2014; Huangfu et al., 2015; Ma et al., 2018). Briefly, the MnO_2 NPs were prepared from equivalent amounts of $Na_2S_2O_3$ and $KMnO_4$ by adding the former dropwise into a rapidly stirred solution of the latter. The final MnO_2 suspension at a concentration of 1 mmol/L (0.087 mg/L) was prepared by diluting the stock solution into a 10 mmol/L $NaNO_3$ solution. The resulting MnO_2 suspension was stored in the dark at 4°C and further sonicated for 15 min prior to each measurement. The hydrodynamic diameter, electrophoretic mobility (EPM) and zeta potential of MnO_2 NPs were determined using a Nano ZetaSizer (Nano ZS90, Malvern, UK) immediately after sonication. The measured average size of the MnO_2 NPs was 58.5 ± 0.6 nm ($n = 30$), their ζ potential was nearly −36.5 mV in 10 mmol/L $NaNO_3$ at pH 6.5 based on at least three different samples for each measurement, and the pH_{IEP} (pH of isoelectric point) was 1.72, nearly consistent with our previous reported value (~1.93) (Jiang et al., 2009). Moreover, the results from dynamic light scattering (DLS) measurements showed that the hydrodynamic diameter of the MnO_2 NPs in an electrolyte solution of 10 mmol/L $NaNO_3$ was determined to be 61–75 nm, which was therefore considered stable to against aggregation during the process of the QCM-D experiments.

1.2. Solution chemistry

Double deionized water (>18.2 MΩ/cm) (ULUPURE Ultrapure Technology Co, Ltd. (China)) was used to prepare all aqueous solutions. The electrolyte stock solution was prepared with analytical reagent-grade $NaNO_3$ with filtration by a 0.22-μm cellulose acetate filter (Whatman ME 24, Middlesex, UK) prior to use. The background electrolyte concentration (10 mmol/L $NaNO_3$) was used for the determination of MnO_2 release for all solutions in this study. The pH for most experiments was unadjusted at pH 6.5 ± 0.5. For the experiments of the influence of solution pH, the pH of the suspension was adjusted to 4.5 and 9.8 with 0.5 mol/L HCl and KOH stock solutions, respectively. Molecular organics (i.e., HA (Fluka no. 53680), alginate (no. V900933) and BSA (no. 180947)) were all obtained from Sigma Aldrich, St. Louis, MO. Stock solutions at the concentrations of 200 mg/L were prepared by filtrating with 0.22-μm syringe filters to remove residual contaminants. The final concentration of organic suspensions was diluted at 5 mg/L to assess the effect of molecules on the release of MnO_2 NPs. All release experiments were conducted at 25°C.

1.3. Release study using a quartz crystal microbalance

To evaluate the release process of MnO_2 nanoparticles from typical surfaces after deposition, a QCM-D system (E4, Q-sense, Biolin Scientific, Sweden) was selected, which was equipped with four modules for the simultaneous measurement of the frequency and dissipation response. MnO_2 NPs were first deposited on a 5 MHz AT-cut crystal surface coated with silica (QSX 303, Q-Sense), magnetite (QSX326) or alumina (QSX 309) in the presence of 10 mmol/L $NaNO_3$. Before each measurement, the QCM crystal sensors were carefully cleaned with the method as described elsewhere. The NP suspension in the electrolyte solution was introduced into the measurement chamber with a slow flow rate of 0.20 mL/min (±0.05 mL/min) to ensure a laminar flow by using a peristaltic pump. The concentration of MnO_2 NPs with background electrolyte suspensions entering the flow modules was maintained at 1 mmol/L. Following the deposition of MnO_2 NPs, the deposited MnO_2 NPs were first thoroughly flushed with a particle-free electrolyte solution of the same solution matrix, followed by DDI water at the same flow rate to induce NP release. For experiments under the influence of macromolecules, a certain amount of HA, alginate or BSA at the final concentration of 5.0 mg/L (total organic carbon, TOC) was added to the mixed suspension containing the same background electrolytes and MnO_2 NPs. With the effect of surface type and solution chemistry, the release behavior of MnO_2 NPs under different conditions leads to an increase in the frequency and a decrease in the dissipative response. Hence, the release rate and degree of MnO_2 NPs from evaluated surfaces can be determined from the rate of frequency shifts during the introduction of DDI water as described in other studies (Quevedo and Tufenkji, 2009; Yi and Chen, 2013; Chowdhury et al., 2014b; Wang et al., 2017). The release process was stopped when the frequency shifts at the third overtone were less than 0.3 Hz in 10 min (Yi and Chen, 2014; Huang et al., 2019).

The frequency shift at nth harmonics (Δf_n; $n = 1, 3, 5, 7, 9, 11, 13$) leads to a positive shift as the remobilization of deposited MnO_2 NPs, follows the Sauerbrey relationship:

$$\Delta m = -\frac{C\Delta f_n}{n} \quad (1)$$

where Δm is the changed mass and C is the crystal constant (17.7 ng/Hz cm^2 for the 5 MHz crystal). Dissipated energy can be described with the dissipation unit (D):

$$D = \frac{E_{\text{dissipation}}}{2\pi E_{\text{stored}}} \quad (2)$$

where $E_{\text{dissipation}}$ is the dissipated energy in one oscillation cycle and E_{stored} is the total energy stored in the oscillator. The changed mass is proportional to the frequency shift when n is fixed from Eq. (1).

2. Results and discussion

2.1. Release of deposited MnO_2 NPs from the silica surface

The frequency and dissipation responses of the crystal sensors at the third harmonics were monitored when MnO_2 NPs were released from the silica-coated crystal surface in 10 mmol/L $NaNO_3$ at pH 6.5, as shown in Fig. 1. Before the measurements, the silica surface was thoroughly rinsed with DDI water to obtain an initial baseline. Following the stable baseline, 10 mmol/L $NaNO_3$ solution was pumped across the surface (stage A). In stage B, a suspension containing MnO_2 NPs with the same concentration of background electrolyte and pH was injected into the measurement chamber. Because the measured frequency shift is proportional to the amount of deposited mass on the silica-coated crystal surface according to the principle of QCM-D (Sauerbrey, 1959), the MnO_2 NP deposition resulted in an increase in the frequency response. Correspondingly, the deposition of MnO_2 NPs enhanced the ability of crystal dissipation which depended on how much was deposited on the crystal surface; thus, the continuous deposition of MnO_2 NPs on the silica surface also led to the observed increase in dissipation. In stage C, the silica surface was subsequently rinsed with 10 mmol/L $NaNO_3$, during which no change in frequency or dissipation was observed, indicating that no deposited MnO_2 NPs were released from the silica surface. When DDI water was introduced into the flow chamber in stage D, however, significant variances in shifts in the frequency and dissipative response were observed, indicating that the release of deposited MnO_2 NPs from the silica surface occurred. The increase in frequency and decrease in dissipation were attributed to the decrease in the deposited mass on crystal surface resulting from the NP release. The result was in agreement with the findings that deposited particles were reversibly attached when the background electrolyte concentration decreased (Jean et al., 1996; Lanphere et al., 2013; Torkzaban et al., 2013; Yi and Chen, 2013; Chowdhury et al., 2014b; Torkzaban and Bradford, 2016). Under these conditions, the negative charge of the MnO_2 NPs and the silica surface were both enhanced due to the reduced charge neutralization effect of DDI water, leading

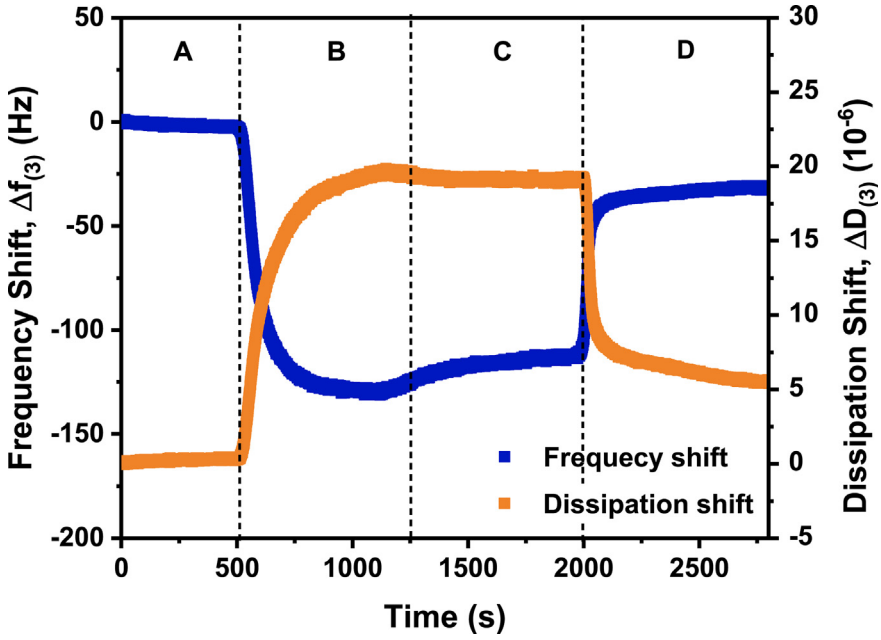

Fig. 1 – Representative frequency and dissipation shifts obtained by QCM-D when MnO_2 NPs are deposited on silica surface at 10 mmol/L $NaNO_3$ and pH 6.5. In Stage A, baselines are obtained by rinsing the silica surface with 10 mmol/L $NaNO_3$ solution. In Stage B, the MnO_2 suspension prepared in 10 mmol/L $NaNO_3$ is introduced, and deposition occurs. In Stage C, the silica surface is rinsed with 10 mmol/L $NaNO_3$ solution. In Stage D, the silica surface is rinsed with DDI water, and MnO_2 NP release takes place.

to lower energy barriers between the two, which was sufficiently small for MnO_2 NPs to be remobilized from silica surface (Ruckenstein and Prieve, 1976). It should be noted that the final Δf was lower than zero, indicating that there were still MnO_2 NPs attached to the surface at the end of the experiment. Similar data had been obtained for ΔD, and there still dissipation in the deposition system.

2.2. *Representative aquatic environmental surface type*

The natural surfaces (e.g., SiO_2, Fe_3O_4 and Al_2O_3) with different compositions and electrostatic properties played a significant role in controlling the release behavior of MnO_2 NPs from the naturally occurring surfaces. The release frequency shift profiles of the MnO_2 NPs from the different surfaces at the third overtone are shown in Fig. 2a. Similar to the release behavior observed from silica surface, the release of MnO_2 NPs from the magnetite and alumina surfaces did not take place until the DDI water (stage D) was injected after the introduction of the electrolyte solution (stage C). However, the amount of deposited MnO_2 NPs on the Fe_3O_4 and Al_2O_3 surfaces was significantly higher than that on the SiO_2 surface, which was observed from the plateau of the frequency profiles in stage B, where deposition occurred. This result could be attributed to the fact that at pH 6.5 in the present study, the SiO_2 and Fe_3O_4 surfaces were both negatively charged, while the Al_2O_3 surface was positively charged (Bahena et al., 2002; Erdemoğlu and Sarıkaya, 2006; Healy, 2006). The less negative surface potential of SiO_2 relative to that of Fe_3O_4 resulted in a weaker electrostatic repulsion between MnO_2 NPs and the Fe_3O_4 surface and thus a higher deposition degree. For the Al_2O_3 surface, the electrostatic attraction between positive Al_2O_3 and MnO_2 with opposite charge created a favorable condition for NP deposition; thus, the highest deposition degree was obtained. The variances in the deposition behavior of MnO_2 NPs on different surfaces can significantly influence the subsequent release in stage D.

The normalized release rates of MnO_2 NPs, determined from the initial slope in the frequency shift measurements, were plotted as a function of surface type in the same solution chemistry in Fig. 2b. Under unfavorable conditions, the release rate of MnO_2 NPs from the SiO_2 surface was nearly 1.98 Hz/s, which was approximately 4 times and 40 times that from the Fe_3O_4 and Al_2O_3 surfaces, respectively. Therefore, it can be concluded that the deposited MnO_2 NPs were most likely released from the silica surface and thus exhibited the highest mobility in the aqueous environment, while the release rate from the alumina surface was nearly zero and the retention of MnO_2 NPs on the alumina surface was almost irreversible. The observed release behaviors of MnO_2 NPs were consistent with the prediction of DLVO theory regarding the interaction of charged particles at different charged surfaces. Previous studies also observed a high release rate of NPs (i.e., quantum dots (QDs) and fullerenes (C_{60})) from the SiO_2 surface (Chen and Elimelech, 2006; Quevedo and Tufenkji, 2009), while the irreversible deposition of MWNTs and partially reversible deposition behavior of graphene oxide (GO) NPs on positively charged Al_2O_3 surfaces (Chang and Bouchard, 2013; Chowdhury et al., 2014b). The findings indicated that the reversibility of MnO_2 NP retention on the environmental surfaces was significantly affected by the surface electrostatic properties, which can influence the interaction between the

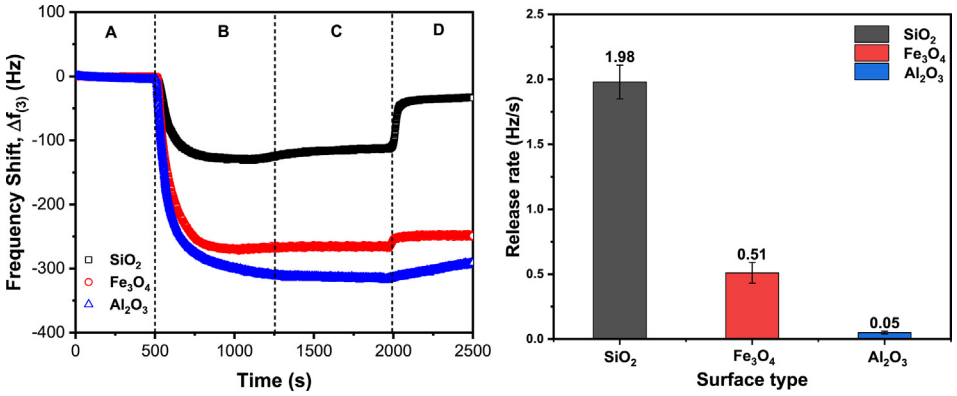

Fig. 2 – (a) Representative frequency and dissipation shifts obtained by QCM-D (from the third overtone measurements) when MnO_2 NPs are deposited on SiO_2, Fe_3O_4 and Al_2O_3 surfaces at 10 mmol/L $NaNO_3$ and pH 6.5. (b) Initial release rates when MnO_2 NPs as a function of surface types at 10 mmol/L $NaNO_3$ and pH 6.5 (the standard deviations obtained from at least two replicate measurements).

particles and surface and thus determine the transport potential and mobility of the nanoparticles in aquatic environments.

2.3. *Solution pH impact on colloidal MnO_2 release*

In natural aquatic systems, the solution chemistry is not invariant, and the change of season, climate or human activities may alter the solution chemistry properties (e.g., solution pH). The release of MnO_2 NPs from the above three surfaces at different solution pH values (i.e., 4.5, 6.5 and 9.8) was estimated in the presence of 10 mmol/L $NaNO_3$, and the frequency profiles at the third harmonics are presented in Fig. 3. At pH 4.5, the deposition rates and the deposited amount of MnO_2 NPs on the three different surfaces were significantly higher than those at pH 6.5 and pH 9.8 in stage B. It was clear that the influence of solution pH on the deposition of MnO_2 NPs was more obvious for the SiO_2 and Fe_3O_4 surfaces as shown in Fig. 3a and 3b, indicating that the retention of MnO_2 NPs on these two surfaces was more susceptible to the changes in solution pH. However, Fig. 3c shows that at pH 4.5 the deposition degree of MnO_2 NPs on the alumina surface was significantly lower than that on the other two surfaces, which was not consistent with the finding that the highest deposition of MnO_2 NPs was observed on the alumina surface at pH 6.5 as shown in Fig. 2a. To the best of our knowledge, there was no energy barrier in the case of the Al_2O_3 surface due to the electrostatic attraction at pH < 8 between MnO_2 NPs and alumina observed in our previous report (Huangfu et al., 2013). However, at a moderate concentration of electrolyte (10 mmol/L $NaNO_3$), small separation distance of the energy well decreased the deposition rate of nanoparticles and the attenuated deposition of MnO_2 NPs was observed on Al_2O_3, resulting from the higher ionic strength (Huangfu et al., 2019; Jiang et al., 2010). These findings indicated that MnO_2 NPs were more likely to attach onto the environmental surfaces and have a lower mobility under acidic conditions, which were also slightly affected from the surface types.

In stage C, no MnO_2 NPs were released from the three surfaces when the electrolyte solution with the same background concentration was introduced into the QCM-D system, consistent with the behavior observed in Fig. 2a. After rinsing with DDI water, the release of MnO_2 NPs occurred under different pH conditions. To further understand the influence of solution pH on the release behavior of MnO_2 NPs from surfaces, the fraction of MnO_2 NPs released from the SiO_2, Fe_3O_4 and Al_2O_3 surfaces at different pH values was calculated from the measured frequency changes, as presented in Fig. 4.

Fractions of MnO_2 NP release from different surfaces increased with increasing solution pH. At pH 9.8, the release fractions of MnO_2 NPs from SiO_2, Fe_3O_4 and Al_2O_3 surfaces were 80.58%, 68.61% and 67.16% respectively, significantly higher than those at pH 4.5, where the release fractions were only 7.13%, 4.4% and 6.22%. The experimental results showed that most of the deposited MnO_2 NPs on environmental surfaces would be released back into the aqueous phase under alkaline conditions, while the deposition on the solid surfaces in the water environment was almost irreversible in the solution with strong acidity. When the solution pH increased from 4.5 to 9.8, the MnO_2 NPs became more negatively charged, and the surface potential was prone to be positive at the same time (Huangfu et al., 2013), which was strictly controlled by DLVO theory. Therefore, the energy barrier between the MnO_2 NPs and the surfaces is expected to increase thus the particles can be readily released from surfaces at pH 9.8. In the study by Yi and Chen (2013) on the release behavior of carbon nanotubes (CNTs) from a silica surface, the release degree of MWNTs at pH 4.0 was much lower than that at pH 7.1 in NaCl solution. The lower release fraction was due to the greater number of deprotonated carboxyl groups on the surface of the MWNTs and thus the more negative surface charge at pH 7.1 than at pH 4.0. The enhancement of electrostatic repulsion between the MWNTs and silica surface at pH 7.1 led to a higher energy barrier height for the MWNTs and the silica surface, namely, a lower energy barrier for MWNT release, and hence a higher degree of release. Therefore, the change in

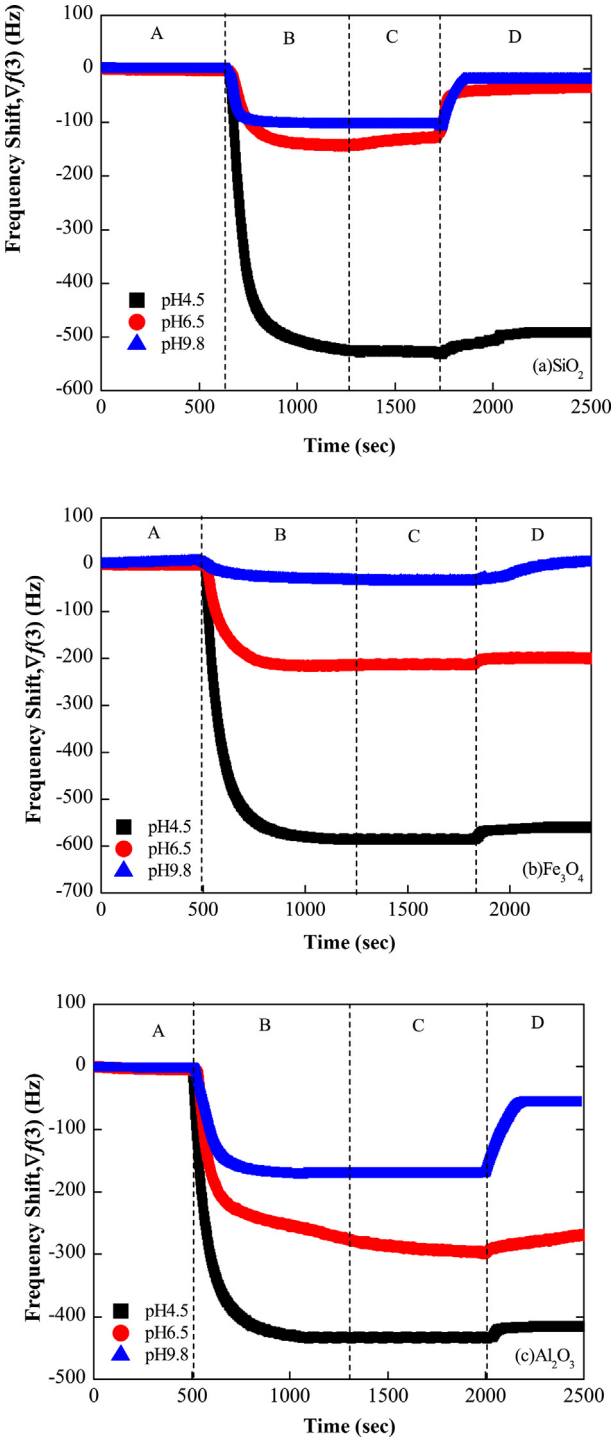

Fig. 3 – Representative frequency shifts obtained by QCM-D when MnO_2 NPs are deposited on (a) SiO_2 (b) Fe_3O_4 and (c) Al_2O_3 surfaces in different pH values in 10 mmol/L $NaNO_3$.

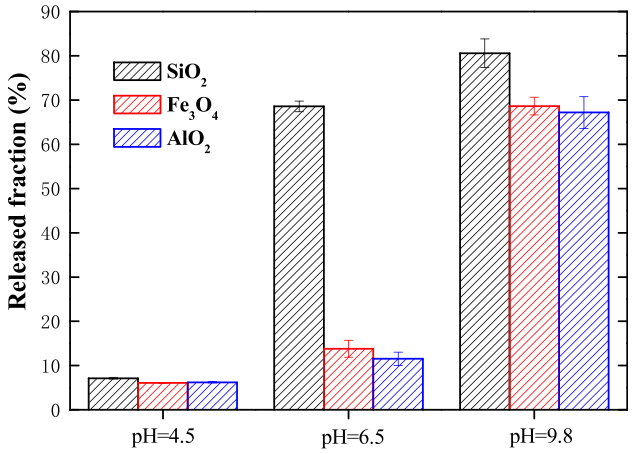

Fig. 4 – Fractions of deposited MnO_2 released from on SiO_2, Fe_3O_4 and Al_2O_3 surfaces at 10 mmol/L $NaNO_3$ and pH 4.5, 6.5 and 9.8.

solution pH can impact the remobilization of nanoparticles deposited on mineral and metal oxide surfaces in the environment by modifying the surface potential of the particles.

2.4. *Influence of macromolecular organic matter*

The release of MnO_2 NPs was also explored in the presence of three model macromolecules (i.e., HA, alginate and BSA), representing humic substances, polysaccharide and protein, respectively, which commonly exist in the water environment. The frequency profiles obtained in 10 mmol/L $NaNO_3$ at pH 6.5 are shown in Fig. 5, and the fractions of released MnO_2 NPs are plotted in Fig. 6. Compared with the release behavior in the absence of organic matter, different macromolecular organics have significant effects on the deposition and release of MnO_2 NPs. In stage B, the presence of BSA significantly increased the deposition degree of the MnO_2 NPs on the three different surfaces, while the addition of HA and alginate inhibited MnO_2 deposition, as shown by the frequency shifts in Fig. 5. The experimental results were consistent with the findings in our previous publication that humic acid and the two biomacromolecules showed different effects on influencing the deposition of MnO_2 colloids and other nanoparticles, dependent on the composition of the organics (Huangfu et al., 2019). In addition, when the mixed suspension containing the same background electrolyte concentration and macromolecular organics was introduced into the flow module, no release of MnO_2 NPs occurred. When DDI water was introduced at stage D, only minimal release of MnO_2 NPs was observed at first (Fig. 5), though continued release occurred and reached a maximum at the end, indicating that the change in solution electrolytic conditions was still the predominant factor determining the release of NPs in three aquatic systems.

Furthermore, the release of MnO_2 NPs in the presence of different molecules showed the opposite effect. In the presence of HA, the release fractions of MnO_2 NPs were the highest, approximately 57%, 51% and 61% for the SiO_2, Fe_3O_4 and Al_2O_3 surfaces, respectively, followed by alginate and those in the absence of molecular organics, while only ~7% deposited MnO_2 was on average released from the three surfaces in the presence of BSA. These results demonstrated that the mobility of MnO_2 NPs can be enhanced in an HA and alginate background, while BSA can hinder the mobility of MnO_2 NPs in the aquatic phase and enhance their retention on environmental surfaces. Moreover, relative to the influence of surface type, the presence of background macromolecular organics exhibited a greater impact on the release behavior of MnO_2

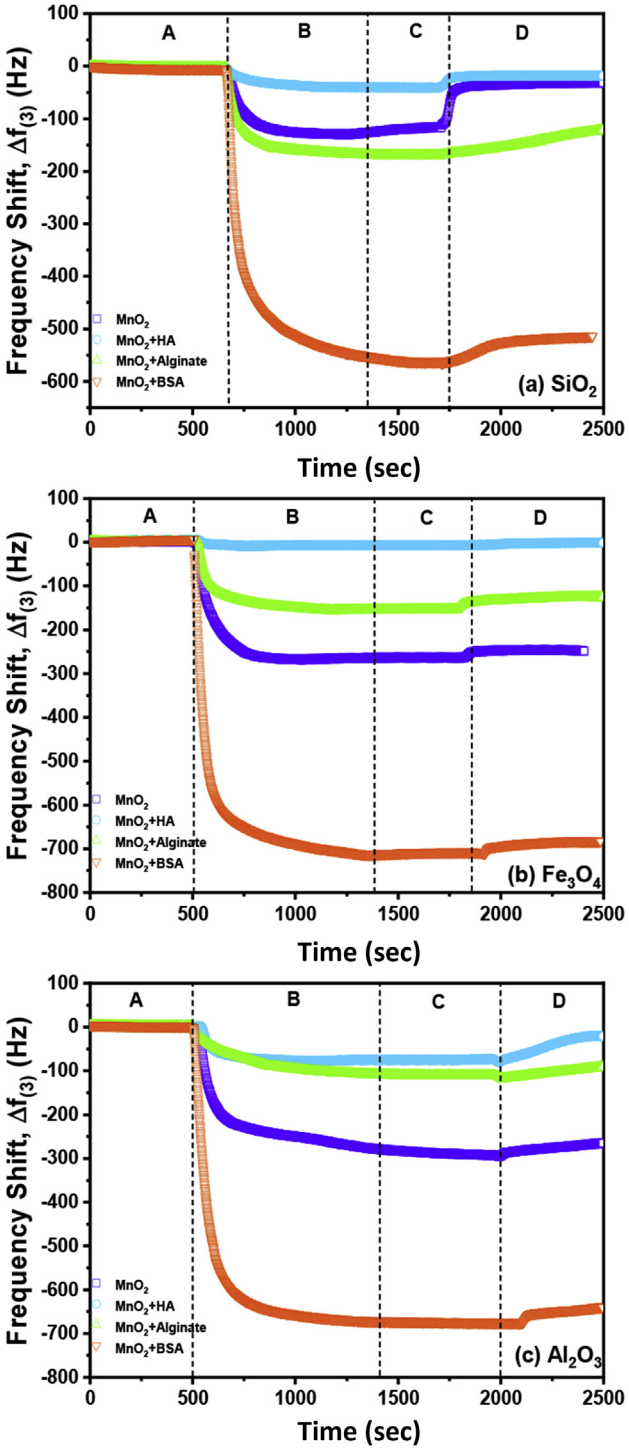

Fig. 5 – Representative frequency shifts obtained by QCM-D when MnO_2 NPs are deposited on SiO_2, Fe_3O_4 and Al_2O_3 surfaces in the absence and presence of HA, alginate and BSA in 10 mmol/L $NaNO_3$ at pH 6.5.

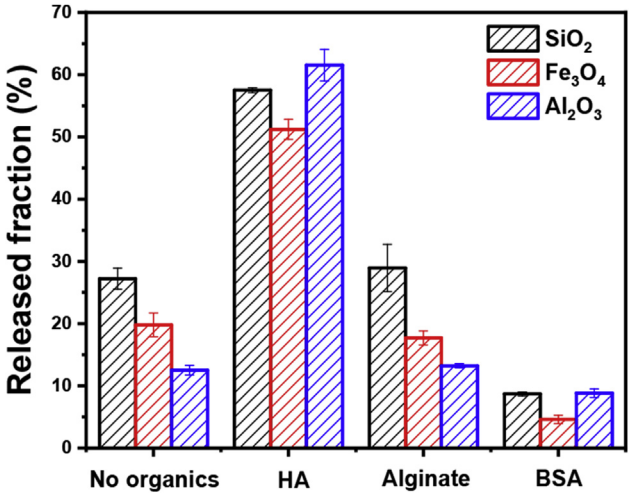

Fig. 6 – Fractions of deposited MnO_2 released from SiO_2, Fe_3O_4 and Al_2O_3 surfaces as a function of macromolecule types at 10 mmol/L $NaNO_3$ and pH 6.5.

NPs. The different effects of the molecular organics on the release of MnO_2 can be attributed to the structural variance of the molecules. There is a large number of functional groups on the HA surface, and its adsorption on the MnO_2 NP surface may lead to a decrease in its ability to contact the deposited surfaces, thus increasing the release fraction. Alginate has a surface with higher surface roughness and more linear structure than that of HA (Kai and Elimelech, 2008), which enabled a tight wrapping of the MnO_2 NPs within the adsorption layer of alginate. This additional physical capture can result in an enhancement in the interaction of MnO_2 NPs with the surface and thus a reduced release degree of MnO_2 NPs relative to HA was obtained. A previous study by Chowdhury et al. also showed a similar effect of humic substances and alginate on the release of GOs from a SiO_2 surface, and similar mechanisms were proposed (Chowdhury et al., 2014c). However, BSA molecules, with a special molecular structure, have a large number of positively charged Lys residues on their surface (Kubiak-Ossowska et al., 2017). The adsorption of BSA on the MnO_2 surface can provide additional deposition sites for MnO_2 NPs (Flynn et al., 2012), and strengthen the connection between MnO_2 and the surface through electrostatic attraction. The deposited MnO_2 NPs need to overcome a high barrier to be released from the surface in the presence of BSA, and the minimum release was therefore observed.

2.5. *Changes in the dissipative properties of the deposited layer*

As MnO_2 NPs deposited onto the crystal surface, the crystal's ability to dissipate energy increased simultaneously with decreasing frequency shifts (Fatisson et al., 2009). The ratio of dissipation slope to frequency shifts ($\left|\frac{\Delta D}{\Delta f}\right|$) can be used as an estimation of the characteristics of the deposited layers on QCM-D crystal sensors (Chang and Bouchard, 2013; Li et al., 2014; Chowdhury et al., 2014b; Chen et al., 2016); a lower value indicates a rigid deposited layer, while a higher value is observed for a dissipative and soft deposited layer (Gall et al., 2013).

$|\Delta D_{(3)}/\Delta f_{(3)}|$ calculated using D and f data from early stage B at the third overtone, as a function of solution pH and molecular organics on the three different environmental

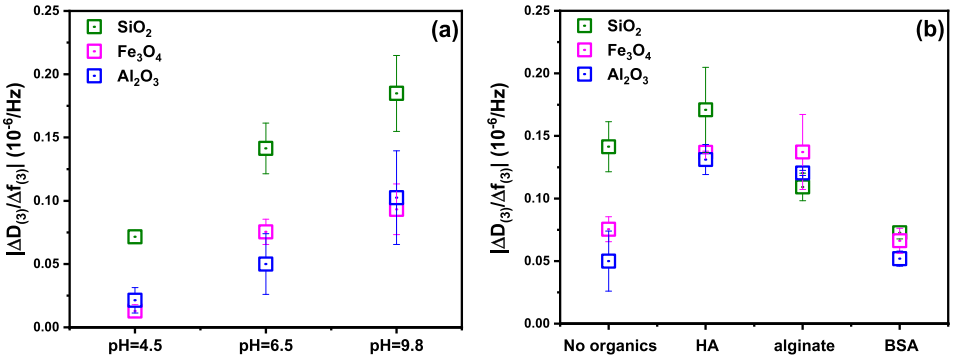

Fig. 7 – (a) Initial $|\Delta D_{(3)}/\Delta f_{(3)}|$ values as a function of solution pH at 10 mmol/L $NaNO_3$ and pH 6.5 on SiO_2, Fe_3O_4 and Al_2O_3 surfaces. (b) Initial $|\Delta D_{(3)}/\Delta f_{(3)}|$ values as a function of as a function of macromolecule types at 10 mmol/L $NaNO_3$ and pH 6.5 on SiO_2, Fe_3O_4 and Al_2O_3 surfaces. Error bars represent standard deviations from at least two measurements.

surfaces, is presented in Fig. 7a and 7b respectively. Overall, the $|\Delta D_{(3)}/\Delta f_{(3)}|$ values in the absence of macromolecules were notably higher (~2.5–3 times) on the silica surface than on the magnetite and alumina surfaces at different solution pH values, indicating that the MnO_2 deposition layers on the silica surface were softer and more dissipative than those of the other two surfaces. Due to the more repulsive interaction for the similarly negative MnO_2 NPs and silica surface, the particles tended to attach loosely on silica surfaces. While under less unfavorable conditions, the deposition of MnO_2 NPs on the magnetite and alumina surfaces was more rigid than that on silica. Similar observations of more rigid nanoparticle deposition on electrostatically favorable surfaces were also reported by previous studies (Chang and Bouchard, 2013; Chowdhury et al., 2014c). The more dissipative the layer was, the more the MnO_2 NPs were likely to be released from the surface. Therefore, the highest release rate and fraction were observed for the silica surface, while a relatively lower release was obtained for the magnetite and alumina surfaces.

Moreover, the $|\Delta D_{(3)}/\Delta f_{(3)}|$ values presented in Fig. 7a were the higher at pH 9.8 for the three surfaces, indicating that MnO_2 deposited layers became softer with increasing solution pH. This soft deposited layer formation in the deposition process under alkaline conditions can be readily released by rinsing with DDI water. The relatively lower $|\Delta D_{(3)}/\Delta f_{(3)}|$ value at pH 4.5 was an indication of rigid layer formation thus the lower release fraction from the surfaces, as observed in Fig. 4. The findings showed that increasing the solution pH can reduce the rigidity of the MnO_2 deposition layers and increase the particle mobility in aquatic systems. In the presence of macromolecules, the $|\Delta D_{(3)}/\Delta f_{(3)}|$ values with background HA were highest, followed by alginate and then BSA. The highest $|\Delta D_{(3)}/\Delta f_{(3)}|$ values on the three surfaces in the presence of HA might be due to the association of MnO_2 NPs with the HA coating instead of their direct association with the solid surfaces, which resulted in a less fully coupled and more dissipative deposited layer, as observed elsewhere (Chang and Bouchard, 2013). However, the low $|\Delta D_{(3)}/\Delta f_{(3)}|$ values were obtained for BSA due to the attractive association of BSA adsorption on the particle surface. This result demonstrated that the attachment of MnO_2 on the crystal surfaces was most rigid in the presence of background BSA, and a higher retention and lower release degree was therefore observed, as shown in Fig. 7b. The findings were in good agreement with our previous study which highlights the role of humic acid and biomacromolecules with regard to MnO_2 NP deposition (Huangfu et al., 2019).

3. Conclusions

After entering the aquatic environment, the transport and mobility of MnO_2 NPs are codetermined by their deposition and release behaviors on environmentally occurring surfaces. The present study reports the release of MnO_2 NPs under various environmentally relevant conditions. The data obtained by using a QCM-D indicated that the release behavior of MnO_2 NPs from the crystal surfaces showed a notable dependence on the surface type, solution pH and background macromolecule. The silica surface showed the highest release rate of MnO_2 due to electrostatic repulsion, followed by the magnetite and alumina surfaces. A high release signified the higher mobility of the MnO_2 NPs in aquatic environments. Solution pH was another critical factor in controlling the reversibility of MnO_2 deposition, with significantly higher release degree from surfaces observed at pH 9.8 than at pH 4.5, indicating that the alkaline conditions were more favorable for the mobilization of MnO_2 in the aquatic environment. In the presence of macromolecular organics, the addition of BSA inhibited the release of MnO_2 due to the attractive regions provided by BSA adsorption, while the presence of HA and alginate enhanced MnO_2 release due to the large repulsive barrier imparted by steric effects. The interpretation of the dissipative properties of the deposited layer provided evidence for the release potential of MnO_2 NPs under different conditions. The findings in the present study will enable a better understanding of the mobility and transport of nanosized MnO_2 particles in aqueous environments.

Conflict of interest

The authors declare that they have no known competing financial interests or personal relationships that could have appeared to influence the work reported in this paper

Acknowledgments

The present work has been financially supported by the National Natural Science Foundation of China (Nos. 51878092, 51608067), the Scientific and Technological Innovation Special Program of Social Livelihood of Chongqing (No. cstc2015shmsztzx0053), and the Fundamental Research Funds for the Central Universities (No. 2019CDXYCH0026).

REFERENCES

Bahena, J.L.R., Cabrera, A.R., Valdivieso, A.L., Urbina, R.H., 2002. Fluoride adsorption onto α-Al2O3 and its effect on the zeta potential at the alumina–aqueous electrolyte interface. Sep. Sci. Technol. 37 (8), 1973–1987.

Buffle, J., Leppard, G.G., 1995. Characterization of aquatic colloids and macromolecules. 1. structure and behavior of colloidal material. Environ. Sci. Technol. 29 (9), 2169–2175.

Chang, X., Bouchard, D.C., 2013. Multiwalled Carbon Nanotube Deposition on Model Environmental Surfaces. Environ Sci Technol 47 (18), 10372–10380.

Chen, K., Elimelech, M., 2006. Aggregation and deposition kinetics of fullerene (C60) nanoparticles. Langmuir 22 (26), 10994–11001.

Chen, Q., Xu, S., Liu, Q., Masliyah, J., Xu, Z., 2016. QCM-D study of nanoparticle interactions. Adv. Colloid Interface Sci. 233, 94–114.

Chowdhury, I., Duch, M.C., Mansukhani, N.D., Hersam, M.C., Bouchard, D., 2014a. Deposition and Release of Graphene Oxide Nanomaterials Using a Quartz Crystal Microbalance. Environ. Sci. Technol. 48 (2), 961–969.

Chowdhury, I., Duch, M.C., Mansukhani, N.D., Hersam, M.C., Bouchard, D., 2014b. Deposition and release of graphene oxide nanomaterials using a quartz crystal microbalance. Environ. Sci. Technol. 48 (2), 961–969.

Chowdhury, I., Duch, M.C., Mansukhani, N.D., Hersam, M.C., Bouchard, D., 2014c. Interactions of Graphene Oxide Nanomaterials with Natural Organic Matter and Metal Oxide Surfaces. Environ. Sci. Technol. 48 (16), 9382–9390.

Erdemoğlu, M., Sarıkaya, M., 2006. Effects of heavy metals and oxalate on the zeta potential of magnetite. J. Colloid Interface Sci. 300, 795–804.

Fatisson, J., Domingos, R.F., Wilkinson, K.J., Tufenkji, N., 2009. Deposition of TiO2 nanoparticles onto silica measured using a quartz crystal microbalance with dissipation monitoring. Langmuir 25 (11), 6062–6069.

Flynn, R.M., Yang, X., Hofmann, T., von der Kammer, F., 2012. Bovine serum albumin adsorption to iron-oxide coated sands can change microsphere deposition mechanisms. Environ. Sci. Technol. 46 (5), 2583–2591.

Gall, I., Herzberg, M., Oren, Y., 2013. The effect of electric fields on bacterial attachment to conductive surfaces. Soft Matter 9 (8).

Healy, T.W., 2006. Colloidal silica: Fundamentals and Application. CRC Press, Boca Raton.

Huang, R.X., Ma, C.X., He, Q., Ma, J., Wu, Z.S., Huangfu, X.L., 2019. Ion specific effects of monovalent cations on deposition kinetics of engineered nanoparticles onto the silica surface in aqueous media. Environ. Sci. Nano 6 (9), 2712–2723.

Huangfu, X., Jiang, J., Lu, X., Wang, Y., Liu, Y., Pang, S.-Y., et al., 2014. Adsorption and Oxidation of Thallium(I) by a Nanosized Manganese Dioxide. Water Air Soil Pollut. 226 (1), 2272.

Huangfu, X., Jiang, J., Ma, J., Liu, Y., Yang, J., 2013. Aggregation Kinetics of Manganese Dioxide Colloids in Aqueous Solution: Influence of Humic Substances and Biomacromolecules. Environ. Sci. Technol. 47 (18), 10285–10292.

Huangfu, X., Ma, C., Huang, R., He, Q., Liu, C., Zhou, J., et al., 2019. Deposition Kinetics of Colloidal Manganese Dioxide onto Representative Surfaces in Aquatic Environments: The Role of Humic Acid and Biomacromolecules. Environ. Sci. Technol. 53 (1), 146–156.

Huangfu, X., Ma, C., Ma, J., He, Q., Yang, C., Jiang, J., et al., 2017a. Significantly improving trace thallium removal from surface waters during coagulation enhanced by nanosized manganese dioxide. Chemosphere 168, 264–271.

Huangfu, X., Ma, C., Ma, J., He, Q., Yang, C., Zhou, J., et al., 2017b. Effective removal of trace thallium from surface water by nanosized manganese dioxide enhanced quartz sand filtration. Chemosphere 189, 1–9.

Huangfu, X.L., Jiang, J., Lu, X.X., Wang, Y., Liu, Y.Z., Pang, S.Y., et al., 2015. Adsorption and Oxidation of Thallium(I) by a Nanosized Manganese Dioxide. Water Air Soil Pollut. 226 (1).

Jean, N.-G., John, E., Tobiason, 1996. Effects of ionic strength on colloid deposition and release. Colloids Surf. A 107 (4), 223–231.

Jiang, J., Pang, S.-Y., Ma, J., 2009. Oxidation of Triclosan by Permanganate (Mn(VII)): Importance of Ligands and In Situ Formed Manganese Oxides. Environ. Sci. Technol. 43 (21), 8326–8331.

Jiang, X.J., Tong, M.P., Li, H.Y., Yang, K., 2010. Deposition kinetics of zinc oxide nanoparticles on natural organic matter coated silica surfaces. J. Colloid Interface Sci. 350 (2), 427–434.

Kai, L.C., Elimelech, M., 2008. Interaction of Fullerene (C60) Nanoparticles with Humic Acid and Alginate Coated Silica Surfaces: Measurements, Mechanisms, and Environmental Implications. Environ. Sci. Technol. 42 (20), 7607–7614.

Kubiak-Ossowska, K., Tokarczyk, K., Jachimska, B., Mulheran, P.A., 2017. Bovine Serum Albumin Adsorption at a Silica Surface Explored by Simulation and Experiment. J. Phys. Chem. B 121 (16), 3975–3986.

Lanphere, J.D., Luth, C.J., Walker, S.L., 2013. Effects of solution chemistry on the transport of graphene oxide in saturated porous media. Environ. Sci. Technol. 47 (9), 4255–4261.

Li, W., Liu, D., Wu, J., Kim, C., Fortner, J.D., 2014. Aqueous Aggregation and Surface Deposition Processes of Engineered Superparamagnetic Iron Oxide Nanoparticles for Environmental Applications. Environ. Sci. Technol. 48 (20), 11892–11900.

Ma, C., Huangfu, X., He, Q., Ma, J., Huang, R., 2018. Deposition of engineered nanoparticles (ENPs) on surfaces in aquatic systems: a review of interaction forces, experimental approaches, and influencing factors. Environ. Sci. Pollut. Res. 25 (33), 33056–33081.

Ma, J., Graham, N., 1996. Controlling the formation of chloroform by permanganate preoxidation-destruction of precursors. J Water Supply Res. T. Aqua. 45 (6), 308–315.

Marafatto, F.F., Lanson, B., Peña, J., 2018. Crystal growth and aggregation in suspensions of δ-MnO2 nanoparticles: implications for surface reactivity. Environ Sci. Nano 5 (2), 497–508.

Markus, A.A., 2016. Release, transport and fate of engineered nanoparticles in the aquatic environment.

Quevedo, I.R., Tufenkji, N., 2009. Influence of solution chemistry on the deposition and detachment kinetics of a CdTe quantum dot examined using a quartz crystal microbalance. Environ. Sci. Technol. 43 (9), 3176–3182.

Ruckenstein, E., Prieve, D.C., 1976. Adsorption and desorption of particles and their chromatographic separation. AIChE J. 22 (2), 276–283.
Sauerbrey, G., 1959. Verwendung von Schwingquarzen zur Wägung dünner Schichten und zur Mikrowägung. Zeitschrift für Physik 155 (2), 206–222.
Torkzaban, S., Bradford, S.A., 2016. Critical role of surface roughness on colloid retention and release in porous media. Water Res. 88, 274–284.
Torkzaban, S., Bradford, S.A., Wan, J., Tokunaga, T., Masoudih, A., 2013. Release of quantum dot nanoparticles in porous media: role of cation exchange and aging time. Environ. Sci. Technol. 47 (20), 11528–11536.
Wang, Z., Wang, X., Zhang, J., Yu, X., Wu, Z., 2017. Influence of Surface Functional Groups on Deposition and Release of TiO2 Nanoparticles. Environ. Sci. Technol. 51 (13), 7467–7475.
Wigginton, N.S., Haus, K.L., Hochella Jr., M.F., 2007. Aquatic environmental nanoparticles. J. Air Wast Mange. 9 (12), 1306–1316.
Yi, P., Chen, K.L., 2013. Influence of solution chemistry on the release of multiwalled carbon nanotubes from silica surfaces. Environ. Sci. Technol. 47 (21), 12211–12218.
Yi, P., Chen, K.L., 2014. Release kinetics of multiwalled carbon nanotubes deposited on silica surfaces: Quartz Crystal Microbalance with Dissipation (QCM-D) measurements and modeling. Environ. Sci. Technol. 48 (8), 4406–4413.